Journal of Materials Chemistry A

Accepted Manuscript

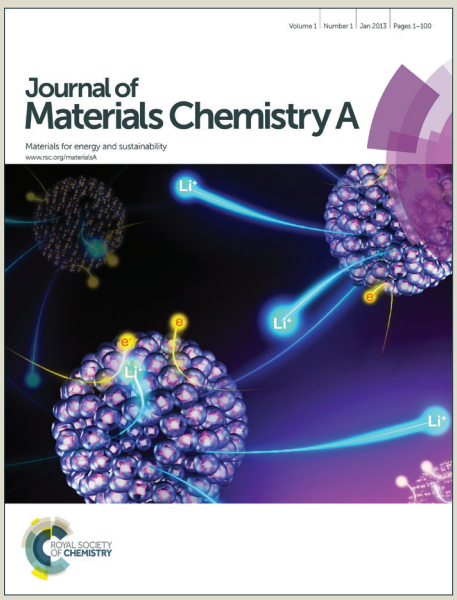

ROYAL SOCIETY OF CHEMISTRY

www.rsc.org/materialsA

Journal of
Materials Chemistry A

RSCPublishing

COMMUNICATION

Graphene nanosheets loaded with Pt nanoparticles with enhanced electrochemical performance for sodium-oxygen batteries

Cite this: DOI: 10.1039/x0xx00000x

Received ooth January 2012,
Accepted ooth January 2012

DOI: 10.1039/x0xx00000x

www.rsc.org/

Sanpei Zhang, Zhaoyin Wen*, Kun Rui, Chen Shen, Yan Lu, Jianhua Yang

Graphene nanosheets loaded with highly dispersed platinum nanoparticles (Pt@GNSs) are prepared by a simple and effective hydrothermal method. Pt@GNSs as air cathode material exhibits a very high initial discharge capacity of 7574mAh/g at the current density of 0.1mA/cm^2 and delivers a stable cycling performance The electrocatalytic characteristic of Pt on Na-O_2 cell is firstly investigated.

The abundance of sodium makes Na-O_2 batteries suitable for large scale application, especially in comparison with the lithium-based batteries due to the limited supply of lithium resource. However, research on Na-O_2 cells is still in an infant stage. Unlike for non-aqueous lithium-oxygen cells where Li_2O_2 is formed, reports on the nature of the discharge product in sodium-oxygen cells are less consistent and different discharge products have been reported.[1] Recently, Hartmann et al. found sodium superoxide (NaO_2) as the discharge product with low overpotential using a carbon-fibre gas diffusion layer as the cathode and sodium triflate salt ($NaSO_3CF_3$) in diethylene glycol dimethyl ether (DEGDME) as electrolyte.[2] In addition, they also studied the impact of the local current density and different type of carbon on the sodium superoxide (NaO_2) battery.[3] Zhao et al. also reported NaO_2 as the discharge product in the static Ar/O_2 (80/20 vol%) using vertically aligned carbon nanotubes as air electrode and sodium triflate salt in tetraethylene glycol dimethyl as electrolyte.[4] However, Jian et al. found $Na_2O_2{\cdot}2H_2O$ as the main product using CNT paper as air electrode and 0.5M $NaSO_3CF_3$/DEGDME as electrolyte.[5] Fu et al. has investigated Na-O_2 cells with carbonate and ether based electrolytes while different carbon materials were used as the air electrode. Their results indicated the formation of sodium peroxide (Na_2O_2) but with a significant fraction of sodium carbonate as a discharge product with the use of either carbonate or ether electrolytes.[6] In a work by Kim et al. using a propylene carbonate (PC) based electrolyte solution (1 M $NaClO_4$) sodium carbonate was the main discharge product. In experiments using tetraglyme with 1 M $NaClO_4$, they found $Na_2O_2{\cdot}2H_2O$ and trace amounts of sodium hydroxide.[7] They proposed different charge/discharge mechanisms with various discharge products. Meanwhile, McCloskey et al. present a comparative study of non-aqueous Li-O_2 and Na-O_2 batteries employing an ether-based electrolyte and found "cleaner" chemistry with lower amount of parasitic products during the charge cycle of the Na-O_2 cell.[8] Their results indicated that Li_2O_2 is more reactive than NaO_2, leading to the observed large charge overpotential. Besides, Lee et al. pointed out that the minimum energy barrier for the NaO_2 decomposition was substantially lower than that of Li_2O_2 decomposition using first-principle calcultation.[9] Kang et al. indicated that NaO_2 is only more stable at nanoscale below 10 nm in particle size by theoretical calculation.[10]

With respect to previous work on Na-O_2 cells the main questions are remained: i) what determines the nature of the discharge product, i.e., the NaO_2, Na_2O_2, $Na_2O_2{\cdot}H_2O$ and Na_2CO_3; ii) in terms of NaO_2 as discharge product, the large overpotential during discharge (η_{dis} > 250 mV), limited discharge capacity and poor cycle performance with cycling limitation mode have been found. iii) the potential gap of Na-O_2 during charge is usually higher than 1 V and poor cycle performance have been found with other sodium compounds as discharge products. The aforementioned studies focused on the impact of electrolyte, type of carbon and testing atmosphere, but only a few on catalysts.

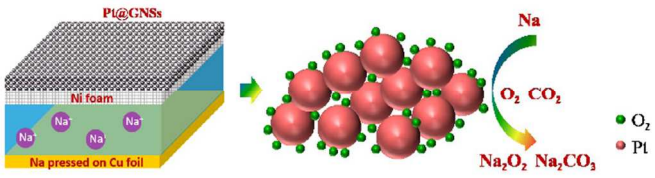

Fig. 1 Schematic for structure and proposed electrocatalytic mechanism of Na-O_2 cell.

Herein, we developed a new bifunctional oxygen electrode with graphene nanosheets as the support and studied the electrochemical

performance of Pt nanoparticles in Na-O_2 cell for the first time. Possible reaction mechanism of the synthesized Pt@GNSs cathode is proposed.

Graphene nanosheets were synthesized by the oxidation of graphite powder using the modified Hummers' method[11]. Then platinum nanoparticles were grown in situ on the graphene nanosheets via a traditional hydrothermal method[12]. Specifically, 60 mg GNSs was dispersed in a mixture of 20 mL ethylene glycol and 1.5 mL 0.1 g/mL H_2PtCl_6 solution. After 30 min ultrasonication treatment, the suspension was transferred into a 50 mL Teflon-lined autoclave and heated at 120°C for 4 hours. Final graphene nanosheets loaded with Pt nanoparticles were then washed thoroughly with water and ethanol and dried at 80°C for 12h under vacuum. As the cell structure schematic shown in Fig. 1, the cathode and anode were separated simply by electrolyte without any separator. The detail of cell assembly was described in the Experimental section in the ESI.†

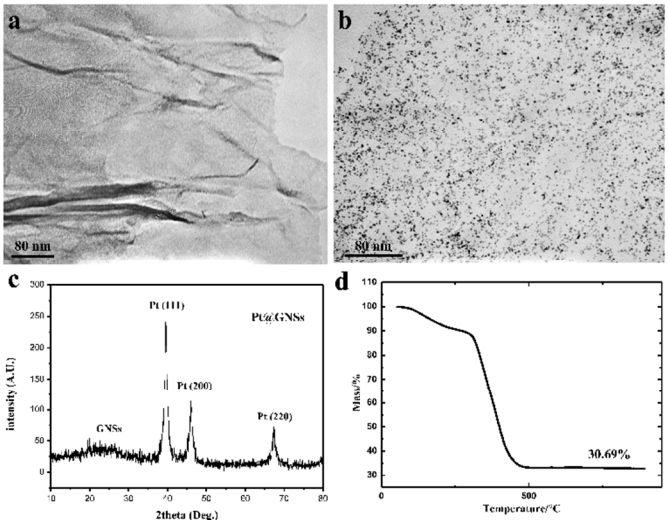

Fig. 2 TEM image of GNSs (a) and Pt@GNSs (b), (c) XRD of Pt@GNSs, (d) TG of Pt@GNSs.

Fig. 2a shows the TEM image of GNSs. Clean and transparent wrinkle sheets are observed, indicating that the graphene nanosheets have been successfully exfoliated from the graphite flake. After the hydrothermal procedure, Pt nanoparticles are homogenously grown on the graphene nanosheets as TEM image indicated (Fig. 2b). The particle size of platinum is found to be ~5nm, which is the catalysts' ideal size for oxygen reduction reaction[13]. To further investigate the structural information of the product, X-ray diffraction (XRD) was carried out. As shown in Fig. 2c, all the diffraction peaks agree well with the standard pattern of Pt@GNSs, revealing the high purity of the product[14]. TG analysis was carried out to identify the chemical composition of Pt@GNSs (Fig. 2d). An obvious weight loss occurred between 250°C and 500°C when the composite was heated in air atmosphere, which was mainly ascribed to the oxidization of carbon generating CO_2. The mass fractions of platinum in Pt@GNSs composite is 30.69% based on the mass loss result.

In order to understand the role of Pt in the oxygen evolution reaction (OER) and oxygen reduction reaction (ORR), we compared the electrochemical performance of Pt@GNSs and GNSs as cathodes for sodium oxygen batteries. Fig. 3a is the first discharge and charge profiles of the Na-O_2 battery. The charge and discharge measurement was carried out at the current density of 0.1mA/cm^2. The specific capacity of the GNSs and Pt@GNSs electrodes is based on the mass of GNSs and the total mass of GNSs and Pt, respectively. The discharge capacity of Pt@GNSs is 7574mAh/g, while only 5413mAh/g for GNSs cathode can be obtained at the same current density. About 40% increase of discharge capacity demonstrates that Pt@GNSs has a much higher OER catalytic activity than that of GNSs. Several reasons are deduced as follows. Firstly, the presence of Pt nanoparticles supplies more oxygen adsorption sites, like a reservoir for oxygen, which benefits the increase of discharge capacity; secondly, uniformly dispersed Pt nanoparticles are conducive to the homogenously deposition of discharge products, which efficiently alleviates the blockage of oxygen diffusion channels due to the discharge product aggregation, leading to a good capacity performance; besides, the good conductivity of Pt nanoparticles is in favours the conductivity of the air electrode especially when they are embedded in insulating discharge products.

Despite the excellent discharge performance due to the Pt nanoparticles, Pt@GNSs cathode exhibited complicated polarization features. Generally speaking, on one hand, initial charge-discharge performance of the air electrodes before and after Pt nanoparticles deposition is not improved distinctly (Fig. 3a). On the other hand, long-time polarization performance after composited with Pt nanoparticles is obviously enhanced by comparing Fig. 3b and 3c. The average discharge voltage plateau is about 2.3V, which is consistent with the theoretical value of Na-O_2 batteries[15]. The charge voltage plateau is ~3.4V, significantly lower than that reported for Na_2O_2 or Na_2CO_3 decomposition[6, 7], which may be ascribed to the specific cell structure design in our present work. Unlike the case in Li-O_2 batteries,[16] the Pt nanoparticles display no evident catalytic activity on decreasing the discharge and charge overpotentials with 1M $NaClO_4$/PC as the electrolyte. However, the Pt@GNSs cathode does display higher electrochemical activity than GNSs for OER process.

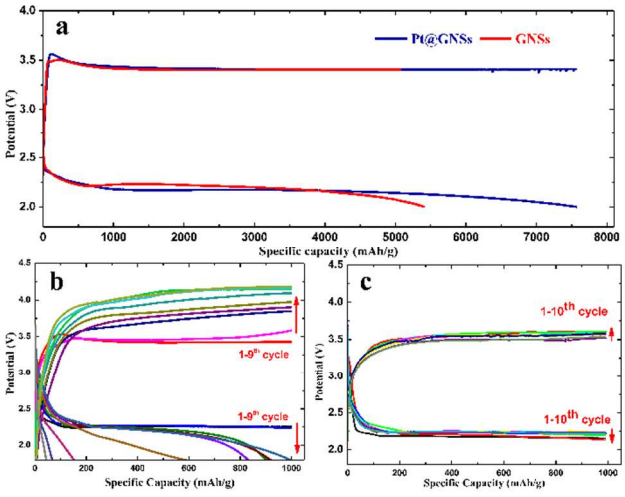

Fig. 3 (a) The discharge/charge profiles of GNSs and Pt@GNSs electrodes, (b) charge and discharge performance of initial 9 cycles of GNSs, (c) charge and discharge performance of initial 10 cycles of Pt@GNSs.

The long-time polarization performance of the two cathodes cycled at a low depth of discharge with a capacity limitation of 1000mAh/g at 0.1mA/cm^2 were investigated, as presented in Fig. 3b and 3c. For GNSs electrode (Fig. 3b), the voltage polarization became serious with dramatically increase of charge voltage upon cycling, especially in the 9th cycle, which is ascribed to the lack of catalyst. Meanwhile, obvious discharge capacity decrease happens after the 2nd cycle. The capacity fading may be caused by the insoluble discharge products accumulation in the porous network of the GNSs cathode[17]. As for Pt@GNSs electrode (Fig. 3c), the

voltage polarization during cycling is inhibited with stable discharge and charge voltage plateaus at about 2.38V and 3.6V, respectively, demonstrating the important role of Pt catalyst in the air electrode. It is deduced that the introduction of Pt nanoparticles may be helpful for the decomposition of the discharge products due to the difference of the oxygen adsorb between Pt and graphene[16].

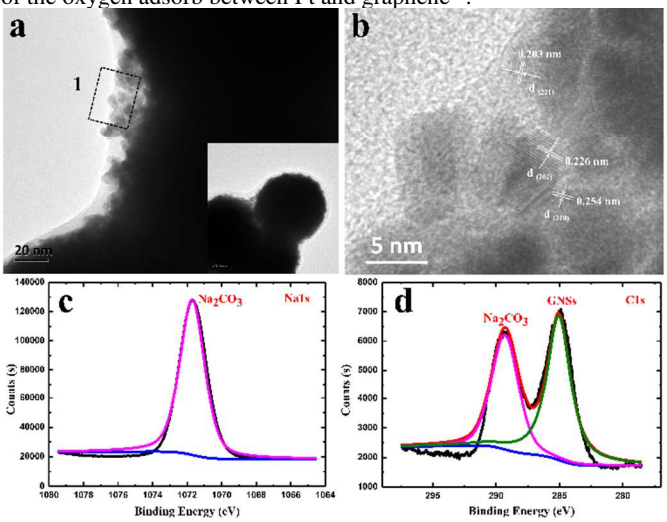

Fig. 4 (a) TEM images of discharge products on the Pt@GNSs cathode , (b) HRTEM image and the corresponding Fourier transform pattern of area 1 in (a), (c) Na1s XPS spectra of the Pt@GNSs as cathode after discharge to 1.8V, (d) C1s XPS spectra of the cathode after discharge to 1.8V.

To obtain deeper insights into the overall electrochemistry and role of Pt, the discharged positive electrodes were harvested and investigated by TEM, FTIR, and XPS. Ex-situ TEM images (Fig. 4a) indicate the formation of discharge products on the positive electrode. The high-resolution transmission electron microscopy (HRTEM) image is shown in Fig. 4b. Interplanar spacings of 2.03 Å, 2.26 Å and 2.54 Å are consistent with the d spacings of (221), (226) and (310) planes of Na_2CO_3, respectively. In addition, the same behaviour was observed with the FTIR spectra shown in Fig. 5. Comparison of electrode materials before and after discharge to 1.8V reveals the characteristic peaks at 1426 cm^{-1} and 879 cm^{-1}, which are corresponding to O-C=O vibrations of Na_2CO_3. Besides, The X-ray photoemission spectroscopy (Fig. 4c and d) presents the Na1s and C1s analysis of the Pt@GNSs cathode after discharge. In the Na1s spectrum, peak at 1071.7eV is assigned to Na_2CO_3.[18] For C1s spectra, peaks at 289.4eV and 285.1eV can be attributed to Na_2CO_3[18] and GNSs[19], respectively. Combining with the ex-situ TEM, FTIR and XPS results, it can be found that the main discharge product is Na_2CO_3[7], which is in agreement with previous reports concerning lithium-oxygen batteries with carbonate based electrolytes[17]. In the $NaClO_4$/PC electrolyte, the highly reactive O_2^- attacks the PC and can, in principle, give rise to a variety of products and react with the Na_2O_2 to form Na_2CO_3.

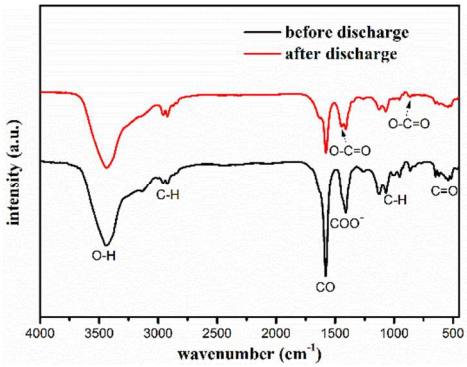

Fig. 5 FTIR spectra of the positive electrode before and after discharge.

Based on the analysis above, a possible reaction mechanism for Na-O_2 cell is proposed (Fig. 1). During the charging process, the Na-O_2 cell electrolyte containing $NaClO_4$/PC electrolyte evolves a certain amount of CO_2 which reacts with the Na_2O_2 to form Na_2CO_3.[7] With the accumulation of insoluble Na_2CO_3, the discharge capacity of GNSs significantly decreases. However, as for Pt@GNSs, oxygen reduction reaction is kinetically preferred on the platinum surface[20]. It may be helpful for Na_2CO_3 to be reduced to Na or other Na-based products.[21] Thus, we deduce that platinum nanoparticles may have a complex effect on the performance of air electrode for Na-O_2 batteries. However, owing to few studies focused on Na-O_2 battery, more experiments should be conducted to further understand the electrolytic mechanism of Na-O_2 batteries.

Conclusions

In summary, the Pt@GNSs are successfully synthesized by a simple hydrothermal method and the platinum nanoparticles are uniformly dispersed on the graphene nanosheets with a particle size of ~5nm. The Pt@GNSs used as cathode showed a high discharge capacity of 7574mAh/g at the current density of 0.1mA/cm^2 and good cycling performance with a limited discharge capacity of 1000mAh/g. Our results demonstrated that the highly dispersed Pt nanoparticles supported by graphene nanosheets possess high electrocatalytic activity for cathode reactions in rechargeable sodium-oxygen batteries. And the complicated catalytic character of platinum in Na-O_2 cells is an interesting and inspiring result.

This work was financially supported by the National Natural Science Foundation of China under Grant No. 51432010 and fundamental research project from the Science and Technology Commission of Shanghai Municipality No. 14JC1493000. We thank Prof. B. V. R. Chowdari (Department of physics, National University of Singapore) for helpful discussion.

Notes and references

[a] *CAS Key Laboratory of Materials for Energy Conversion, Shanghai Institute of Ceramics, Chinese Academy of Sciences, Shanghai 200050, P. R. China. Fax: +86-21-52413903; Tel: +86-21-52411704; E-mail: zywen@mail.sic.ac.cn*

† Electronic Supplementary Information (ESI) available: Experimental section and detail of cell structure. See DOI: 10.1039/c000000x/

1. S. K. Das, S. Lau and L. Archer, *Journal of Materials Chemistry A*, 2014.
2. P. Hartmann, C. L. Bender, M. Vracar, A. K. Duerr, A. Garsuch, J. Janek and P. Adelhelm, *Nat Mater*, 2013, **12**, 228-232.

3. C. L. Bender, P. Hartmann, M. Vračar, P. Adelhelm and J. Janek, *Advanced Energy Materials*, 2014.
4. N. Zhao, C. Li and X. Guo, *Physical Chemistry Chemical Physics*, 2014.
5. Z. L. Pan, Y. Chen, F. J. Li, T. Zhang, C. Liu and H. S. Zhou, *J Power Sources*, 2014, **251**, 466-469.
6. W. Liu, Q. Sun, Y. Yang, J.-Y. Xie and Z.-W. Fu, *Chem Commun*, 2013, **49**, 1951-1953.
7. J. Kim, H.-D. Lim, H. Gwon and K. Kang, *Physical Chemistry Chemical Physics*, 2013, **15**, 3623-3629.
8. B. D. McCloskey, J. M. Garcia and A. C. Luntz, *The Journal of Physical Chemistry Letters*, 2014, **5**, 1230-1235.
9. B. Lee, D. H. Seo, H. D. Lim, I. Park, K. Y. Park, J. Kim and K. Kang, *Chem Mater*, 2014, **26**, 1048-1055.
10. S. Kang, Y. Mo, S. P. Ong and G. Ceder, *Nano Letters*, 2014, **14**, 1016-1020.
11. W. S. Hummers Jr and R. E. Offeman, *J Am Chem Soc*, 1958, **80**, 1339-1339.
12. S. H. Joo, S. J. Choi, I. Oh, J. Kwak, Z. Liu, O. Terasaki and R. Ryoo, *Nature*, 2001, **412**, 169-172.
13. M. Valden, X. Lai and D. W. Goodman, *Science*, 1998, **281**, 1647-1650.
14. S. M. Choi, M. H. Seo, H. J. Kim and W. B. Kim, *Carbon*, 2011, **49**, 904-909.
15. Q. Sun, Y. Yang and Z.-W. Fu, *Electrochem Commun*, 2012, **16**, 22-25.
16. Y. C. Lu, H. A. Gasteiger, E. Crumlin, R. McGuire and Y. Shao-Horn, *J Electrochem Soc*, 2010, **157**, A1016-A1025.
17. S. A. Freunberger, Y. H. Chen, Z. Q. Peng, J. M. Griffin, L. J. Hardwick, F. Barde, P. Novak and P. G. Bruce, *J Am Chem Soc*, 2011, **133**, 8040-8047.
18. A. K.-V. Alexander V. Naumkin, Stephen W. Gaarenstroom, and Cedric J. Powell, Last updated: September 15, 2012 (Created: June 06, 2000).
19. D. Yang, A. Velamakanni, G. Bozoklu, S. Park, M. Stoller, R. D. Piner, S. Stankovich, I. Jung, D. A. Field and C. A. Ventrice Jr, *Carbon*, 2009, **47**, 145-152.
20. N. Markovic, T. Schmidt, V. Stamenkovic and P. Ross, *FUEL CELLS-WEINHEIM-*, 2001, **1**, 105-116.
21. S. K. Das, S. Xu and L. A. Archer, *Electrochem Commun*, 2013, **27**, 59-62.

